Soft-Landed Protein Voltammetry: A Tool for Redox Protein Characterization

ARTICLE *in* ANALYTICAL CHEMISTRY · JULY 2008

Impact Factor: 5.64 · DOI: 10.1021/ac8005389 · Source: PubMed

7 AUTHORS, INCLUDING:

Gabriele Favero
Sapienza University of Rome
75 PUBLICATIONS **471** CITATIONS
SEE PROFILE

Alessandra Tata
University Health Network
26 PUBLICATIONS **232** CITATIONS
SEE PROFILE

Nunzio Tuccitto
University of Catania
39 PUBLICATIONS **511** CITATIONS
SEE PROFILE

Antonino Licciardello
University of Catania
109 PUBLICATIONS **1,502** CITATIONS
SEE PROFILE

Anal. Chem. **2008,** *80,* 5937–5944

Soft-Landed Protein Voltammetry: A Tool for Redox Protein Characterization

Franco Mazzei,*,† Gabriele Favero,† Marco Frasconi,† Alessandra Tata,† Nunzio Tuccitto,‡ Antonino Licciardello,‡ and Federico Pepi*,†

Dipartimento di Chimica e Tecnologie del Farmaco, "Sapienza" Università di Roma, Piazzale Aldo Moro 5, 00185 Roma, Italy, and Dipartimento di Scienze Chimiche, Università degli Studi di Catania, Viale Andrea Doria 6, 95125 Catania, Italy

Microperoxidase-11 (MP-11) was first soft landed onto the gold surface of a screen-printed electrode. Intact protein deposition was verified by time-of-flight secondary ion mass spectrometry. The coupling of soft landing with electrochemical techniques allowed unique information to be obtained about the deposition features. A full characterization of the direct electron-transfer properties was performed by modeling data obtained from cyclic voltammetry experiments; calculated values of kinetic electron-transfer constant, formal redox potential, and reorganization energy allow us to hypothesize the mechanism involved in soft landing immobilization and demonstrate the different conformation of the enzyme deposited from two different charged species. The strong interaction between MP-11 and the gold surface and long-term stability of the functionalized electrode characterizes the peculiar features of this procedure, which enhance its power with respect to the existing immobilization procedure and ensure its suitability for those practical applications that could benefit from an unmediated bridgeless bioeletrochemical electron transfer (e.g., biosensor transducers or electrode elements in biofuel cells).

Electrical contacting between redox proteins and electrode support has attracted substantial research efforts, in particular directed toward understanding the electron-transfer (ET) mechanisms involved in biological systems.[1,2] Direct and mediated protein electron transfer is fundamental in several applications such as biochips,[3] biosensors,[4] and biofuel cells[5,6] where the redox protein must be immobilized on the electrode surface. The approach to the study of direct electron transfer requires interfaces that exhibit fast electron-transfer kinetics together with biocompatibility, that is, without denaturation. Since direct contact between redox enzymes and the bare electrode surface leads to substantial structural or functional changes in the enzyme,[7,8] in the past couple of decades, a burst of research activity has been directed toward the development of immobilization procedures able to create accessible electron-transfer interfaces.[9,10] Recently, we briefly reported a new experimental procedure, called "soft landing protein voltammetry" (SLPV), in which the coupling of ion soft landing with voltammetric techniques has proven to be particularly useful in functionalizing and characterizing protein modified electrode surfaces.[11] Ion soft landing is a mass spectrometric technique based on the deposition at low kinetic energies of specific molecular ions on a solid surface. Since the discovery

* To whom correspondence should be addressed. E-mail: Federico.Pepi@uniroma1.it. Tel.: +390649913119. Fax: +390649913602. E-mail: Franco.Mazzei@uniroma1.it. Tel.: +390649913225. Fax: +390649913133.

† "Sapienza" Università di Roma.

‡ Università degli Studi di Catania.

(1) (a) Armstrong, F. A.; Heering, H. A.; Hirst, J. *J. Chem. Soc. Rev.* **1997**, *26*, 169–179. (b) Rusling, J. F. *Acc. Chem. Res.* **1998**, *31*, 363–369. (c) Jeuken, L. J. C. *Biochim. Biophys. Acta* **2003**, *1604*, 67–76. (d) Vincent, K. A.; Parkin, A.; Armstrong, F. A. *Chem. Rev.* **2007**, *107*, 4366–4413.

(2) (a) Bradley, A. L.; Chobot, S. E.; Arciero, D. M.; Hooper, A. B.; Elliott, S. L. *J. Biol. Chem.* **2004**, *279*, 13297–13300. (b) Armstrong, F. A. *Curr. Opin. Chem. Biol.* **2005**, *9*, 110–117. (c) Léger, C.; Lederer, F.; Guiarelli, B.; Bertrand, P. *J. Am. Chem. Soc.* **2006**, *128*, 180–187. (d) Alcantara, K.; Munge, B.; Pendon, Z.; Frank, H. A.; Rusling, J. F. *J. Am. Chem. Soc.* **2006**, *128*, 14930–14937. (e) Basova, L. V.; Kurnikov, I. V.; Wang, L.; Ritov, V. B.; Belikova, N. A.; Vlasova, I. I.; Pacheco, A. A.; Winnica, D. E.; Peterson, J.; Bayir, H.; Waldeck, D. H.; Kagan, V. E. *Biochemistry* **2007**, *46*, 3423–3434. (f) Fourmond, V.; Lagoutte, B.; Sétif, P.; Leibl, W.; Demaille, C. *J. Am. Chem. Soc.* **2007**, *129*, 9201–9209. (g) Prytkova, T. R.; Kurnikov, I. V.; Beratan, D. N. *Science* **2007**, *315*, 622–625.

(3) Zhu, H.; Snyder, M. *Curr. Opin. Chem. Biol.* **2002**, *7*, 55–63.

(4) (a) Willner, I.; Katz, E. *Angew. Chem., Int. Ed.* **2000**, *39*, 1180–1218 (b) Armstrong, F. A.; Wilson, G. S. *Electrochim. Acta* **2000**, *45*, 2623–2645 (c) Willner, I.; Baron, R.; Willner, B. *Biosens. Bioelectron.* **2007**, *22*, 1841–1852. (d) Katz, E.; Shipway, A. N.; Willner, I. In Bioelectrochemistry; Wilson, G. S., Bard, A. J., Stratmann, M., Eds.; *Encyclopedia of Electrochemistry*; Wiley-VCH; Weinheim, Germany, 2002; *Vol. 9*,Chapter 17, pp 559−626.

(5) (a) Willner, I. *Science* **2002**, *298*, 2407–2408. (b) Katz, E.; Lioubachevski, O.; Willner, I. *J. Am. Chem. Soc.* **2005**, *127*, 3979–3988 (c) Katz, E.; Shipway, A. N.; Willner, I. In *Handbook of Fuel Cell Technology*; Vielstich, W., Gasteiger, H., Eds; Willey: Chichester, 2002; Vol. 1, Part 4, Chapter 21, pp 355−381. (d) Katz, E. In *2004 Yearbook of Science and Technology*; Blumel, D., Ed.; McGraw-Hill Professional: New York, 2004; pp 33−37.

(6) (a) Mano, N.; Mao, F.; Heller, A. *J. Am. Chem. Soc.* **2002**, *124*, 12962–12963. (b) Soukharev, C.; Mano, N.; Heller, A. *J. Am. Chem. Soc.* **2004**, *126*, 8368–8369. (c) Calabrese Barton, S.; Gallaway, J.; Atanassov, P. *Chem. Rev.* **2004**, *104*, 4867–4886. (d) Heller, A. *Phys. Chem. Chem. Phys.* **2004**, *6*, 209–216. (e) Kamikata, Y.; Tsujimura, S.; Setoyama, N.; Kajino, T.; Kano, K. *Phys. Chem. Chem. Phys.* **2007**, *9*, 1793–1801.

(7) Holt, R. E.; Cotton, T. M. *J. Am. Chem. Soc.* **1989**, *111*, 2815–2821.

(8) Heller, A. *Acc. Chem. Res.* **1990**, *23*, 128–134.

(9) (a) Lvov, Y. M.; Lu, Z.; Schenkman, J. B.; Zu, Z.; Rusling, J. F. *J. Am. Chem. Soc.* **1998**, *120*, 4073–4081. (b) Swatloski, R. P.; Spear, S. K.; Holbrey, J. D.; Rogers, R. D. *J. Am. Chem. Soc.* **2002**, *124*, 4974–4982. (c) Zhang, Z.; Chouchane, S.; Magliozzo, P.; Rusling, J. F. *Anal. Chem.* **2002**, *74*, 163–170. (d) Lu, Q.; Hu, C.; Cui, R.; Hu, S. *J. Phys. Chem. B* **2007**, *111*, 9808–9813.

(10) (a) Chi, Q.; Zhang, J.; Andersen, J. E. T.; Ulstrup, J. *J. Phys. Chem. B* **2001**, *105*, 4669–4679. (b) Rivas, L.; Turgida, D. H.; Hildebrandt, P. *J. Phys. Chem. B* **2002**, *106*, 4823–4830. (c) Heering, H. A.; Wiertz, F. G. M.; Dekker, C.; de Vries, S. *J. Am. Chem. Soc.* **2004**, *126*, 11103–11112. (d) Nakano, K.; Yoshitake, T.; Yamashita, Y.; Bowden, E. F. *Langmuir* **2007**, *23*, 6270–6275.

(11) Pepi, F.; Ricci, A.; Tata, A.; Favero, G.; Frasconi, M.; Delle Noci, S.; Mazzei, F. *Chem. Commun.* **2007**, 3494–3496.

10.1021/ac8005389 CCC: $40.75
Published on Web 06/25/2008

that ion storage is possible on a structurally organized self-assembled monolayer (SAM),[12] this technique has been enhanced and has enabled organic ions,[13] DNA fragments,[14] and proteins[15] to be collected on different surfaces. Covalent immobilization of mass-selected peptides on SAM surfaces has recently been demonstrated.[16]

In this work, we report an extended characterization of protein deposition onto gold surfaces by SLPV and time-of-flight secondary ion mass spectrometry (TOF-SIMS) procedures. For this purpose, we used microperoxidase-11 (MP-11), an undecapeptide derived from the enzymatic cleavage of cytochrome *c*, which retains its peroxidase activity. MP-11 catalyzes the oxidation of a wide range of organic substrates exhibiting a reversible electrochemical behavior of the heme Fe^{II}/Fe^{III} couple. The immobilization of intact MP-11 has been verified by TOF-SIMS experiments. To demonstrate the validity of this deposition technique, native structural and reactivity characteristics of the protein must be maintained; to this end, exciting opportunities are afforded by using electrochemical methods. In this article, we consider cyclic voltammetry, which although generally considered as a qualitative technique with regard to electron-transfer kinetics, is highly suited to visualizing and analyzing coupling processes. Most of the knowledge on proteins' ET has been gleaned from transient kinetics studies of reaction centers. According to Marcus' theory, the ET rate to and from an electrode increases exponentially with a modest electrochemical driving force and then levels off to a maximum value at a sufficiently large overpotential:[17,18] this enables key parameters such as long-range electronic coupling (distance and medium dependence) and Franck−Condon reorganization terms to be examined in detail. Hereafter, we provide the first rigorous and fully analytical treatment of the kinetics of reversible ET of a soft-landed protein. In order to verify the retention of the biocatalytic activity of soft-landed microperoxidase, a series of electrochemical experiments were also performed in the presence of hydrogen peroxide as substrate.

Moreover, the reported procedure can be scaled down to interrogate other more complex redox protein-electrode systems.

EXPERIMENTAL SECTION

The soft landing of mass-selected ions was achieved using a TSQ700 triple quadrupole from Thermo Finnigan Ltd., modified as previously reported.[11]

Sample ionization was performed in the TSQ700 ESI source by operating in the following conditions: needle voltage 4.0 kV, flow rate 20 μL min^{-1}, capillary temperature 423 K, capillary exit and skimmer voltage 40 and 90 V, respectively, and hexapole dc offset −0.8 V.

Solutions of MP-11 were prepared daily in 1:1 H_2O/CH_3OH, 1% CH_3COOH at a concentration of $\sim10^{-4}$ M.

The ion dose was measured by monitoring the ion current on the electrode surface using a Keithley Instruments Picoammeter. Typical ion current measurements are 50−150 pA.

The ion beam is collimated onto the working electrode of a screen-printed electrode (cod. AC1.W1.R1) purchased from BVT Technologies, (Brno, Czech Republic). The sensor is constituted by a gold surface (as working electrode, 1-mm diameter), an Ag/AgCl reference electrode (198 mV vs NHE), and a gold counter electrode. The electrochemical measurements are performed in 0.05 M phosphate buffer solution pH 7.0, with 0.1 M KCl, at different scan rates using a thermostatted electrochemical cell under nitrogen stream with a μAutolab (from EcoChemie, Utrecht, The Netherlands).

TOF-SIMS measurements were performed using a reflector-type spectrometer (ION-TOF TOFSIMS IV, Muenster, Germany) with a pulsed Bi_3^{2+} primary ion beam (25 kV, ∼0.05 pA). Primary ion fluence was kept at $<3 \times 10^{11}$ ions cm^{-2} in order to ensure static SIMS conditions.[19] Large area images (8 mm × 8 mm) of the electrodes were acquired in the so-called macroraster mode, by combining the electrostatic rastering of the primary ion beam (125 μm × 125 μm) with the mechanical displacement of the sample carried out using a stepper−motor-driven sample manipulator.

To better characterize the ion spot width, screen-printed electrodes having a 4-mm diameter working gold electrode (Dropsense, Oviedo, Spain) were used for the TOF-SIMS experiments.

RESULTS AND DISCUSSION

Soft-Landing Experiments. The ESI spectrum of the acid solution of MP-11 displays similar intensities of $[MP\text{-}11 + H]^{2+}$ and $[MP\text{-}11 + 2H]^{3+}$ ions. The ferric−heme moiety brings one positive charge whereas two protons, presumably bound to the peptide's amino groups, are responsible for the additional positive charges. The whole unresolved isotopic pattern corresponding to $[MP\text{-}11 + H]^{2+}$ and $[MP\text{-}11 + 2H]^{3+}$ ions, respectively, is mass-selected with the first quadrupole and soft-landed on a screen-printed sensor for different time periods ranging from 30 min to 6 h. The mean kinetic energy of the ion beam leaving the third quadrupole are measured by using the cutoff potential and can be estimated as 10−12 eV. An additional acceleration potential, ranging from 0 to −200 V, is applied to the working gold electrode in order to guide the ions to the surface. The applied potential is a critical feature in obtaining a suitable deposition of the peptide on the target metal surface.

In a typical experiment involving the $[MP\text{-}11 + H]^{2+}$ ions, a current of 50−150 pA is measured at the surface. The rough estimation of the ion current is due to the high noise registered by the picoammeter, probably due to the shieldless surface introduction system.

To estimate the ion beam width, different surfaces having a central round hole 0.5−3 mm in diameter were utilized. The ion beam intensity is practically unaffected by passing through the 2.5-mm hole.

(12) Miller, S. A.; Luo, H.; Pachuta, S. J.; Cooks, R. G. *Science* **1997**, *275*, 1447.
(13) (a) Luo, H.; Miller, S. A.; Cooks, R. G.; Pachuta, S. J. *Int. J. Mass Spectrom.* **1998**, *174*, 193–217. (b) Geiger, R. J.; Melnyk, M. C.; Busch, K. L.; Bartlett, M. G. *Int. J. Mass Spectrom.* **1999**, *182/183*, 415–422.
(14) Feng, B.; Wunschel, D. S.; Masselon, C. D.; PasaTolic, L.; Smith, R. D. *J. Am. Chem. Soc.* **1999**, *121*, 8961–8962.
(15) (a) Ouyang, Z.; Takáts, Z.; Blake, T. A.; Gologan, B.; Guymon, A. J.; Wiseman, J. M.; Oliver, J. C.; Davisson, J. A.; Cooks, R. G. *Science* **2003**, *301*, 1351–1354. (b) Blake, T. A.; Ouyang, Z.; Wiseman, J. M.; Takáts, Z.; Guymon, A. J.; Kothari, S.; Cooks, R. G. *Anal. Chem.* **2004**, *76*, 6293–6305. (c) Volný, M.; Elam, W. T.; Ratner, B. D.; Tureček, F. *Anal. Chem.* **2005**, *77*, 4846–4853. (d) Volný, M.; Tureček, F. *J. Mass. Spectrom.* **2006**, *41*, 124–126.
(16) Wang, P.; Hadjar, O.; Laskin, J. *J. Am. Chem. Soc.* **2007**, *129*, 8682–8683.
(17) Chidsey, C. E. D. *Science* **1991**, *251*, 919–922.
(18) Hirst, J.; Armstrong, F. A. *Anal. Chem.* **1998**, 5062–5071.
(19) Benninghoven, A. *Angew. Chem., Int. Ed. Engl.* **1994**, *33*, 1023.

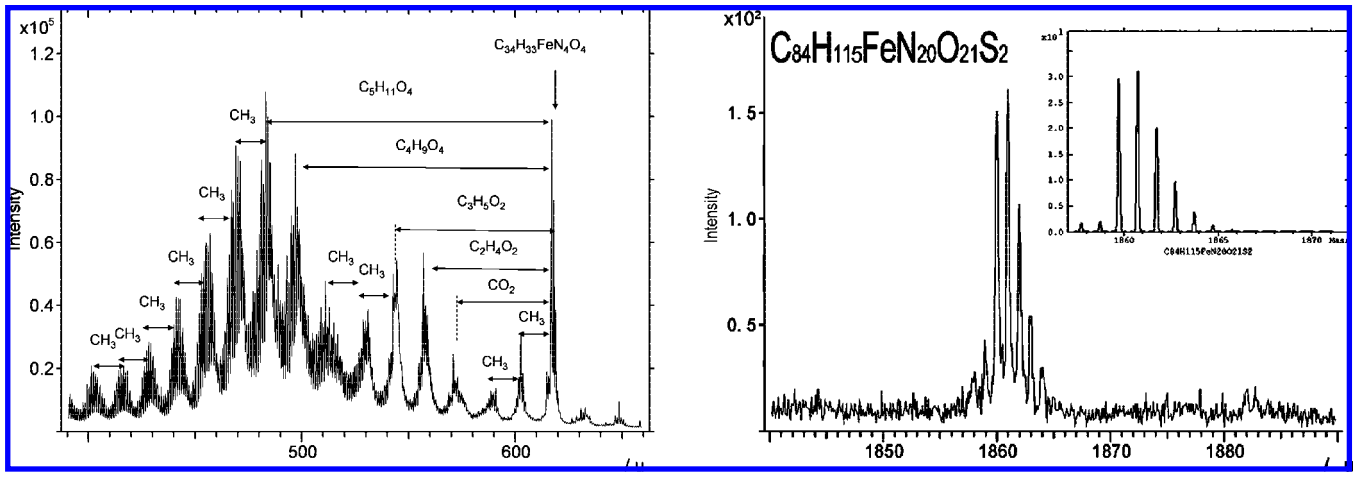

Figure 1. High-mass portion of the TOF-SIMS spectrum of a soft-landed MP-11 layer on gold, showing the presence of fragment peaks characteristic of the heme group (left-hand side) as well as the (quasi) molecular peak (right-hand side of the figure). The inset shows the calculated isotopic distribution expected for a ($C_{84}H_{115}FeN_{20}O_{21}S_2$) ion.

TOF-SIMS Analysis. MP-11 layers deposited by soft landing $[MP\text{-}11 + H]^{2+}$ and $[MP\text{-}11 + 2H]^{3+}$ ions onto a 4-mm-diameter gold surface of a screen-printed electrode were analyzed by TOF-SIMS. Two high mass portions of the typical TOF-SIMS spectrum are displayed in Figure 1. In particular, the (quasi) molecular peak of MP-11 ($C_{84}H_{115}FeN_{20}O_{21}S_2$) is detected, as well as some characteristic heme-related molecular fragments in the mass range 400−650 Da.

The results shown in Figure 1 provide clear evidence that the soft-landing deposition preserves the integrity of the MP-11 molecules. Further important information obtained from TOF-SIMS measurements is related to the spatial distribution of the MP-11 molecule on the electrode surfaces. Indeed, the technique is well suited for providing chemical maps of the surface. Figure 2 shows the mass resolved images of Ag^+ (107 Da), Au^+ (197 Da), and $C_{34}H_{33}FeN_4O_4^+$ (617 Da) acquired over a field of view of 8 mm^2 from a MP-11 deposited electrode. A false-color overlay of the three images is provided as well. The images show that MP-11 is mostly deposited onto the central gold electrode where acceleration potential has been applied, although a weak signal is present also on the outer electrode. It must be emphasized that the images shown in Figure 2 were obtained from the soft-landed electrodes after a strong rinsing in ultrapure water without any significant variation in MP-11 distribution compared with that obtained from the nonrinsed electrode (not shown in the figure). The resistance to rinsing of the soft-landed MP-11 layer provides strong evidence of stable surface anchoring of the molecule. Similar TOF-SIMS results were obtained from the deposition of the two different MP-11 charged ions.

Cyclic Voltammetric Analysis. A thorough investigation of the redox properties of soft-landed MP-11 was performed by cyclic voltammetry. The voltammograms of MP-11 obtained by soft-landing $[MP\text{-}11 + H]^{2+}$ (named in the following **MP-11a**) and $[MP\text{-}11 + 2H]^{3+}$ (named in the following **MP-11b**) are shown in Figure 3. The dependence of anodic and cathodic peak currents versus the potential scan rate confirms the immobilization of the redox protein (data not shown). The formal potential value for **MP-11a** ($E^0 = -80$ mV vs NHE) falls very close to the value

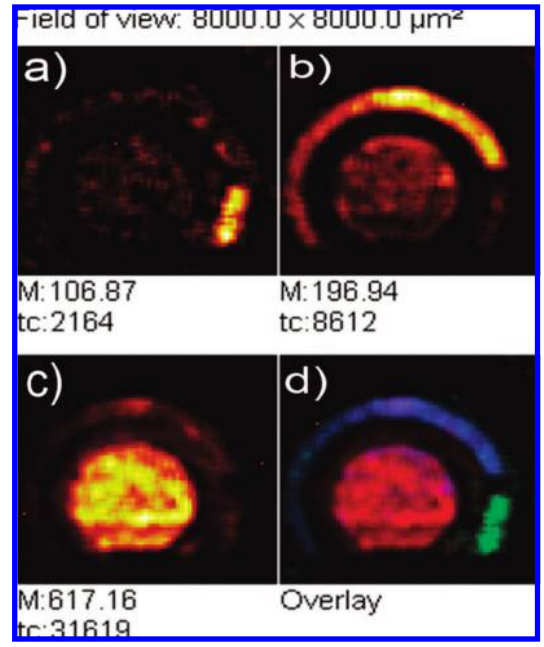

Figure 2. TOF-SIMS mass resolved images of the MP-11 deposited electrode: (a) Ag^+ (mostly from the reference electrode), (b) Au^+, and (c) heme fragment. The false color overlay (d) of the three mass resolved maps (Ag, green; Au, blue; heme, red) indicates that the MP-11 molecule is mostly deposited on the central gold electrode.

reported in the literature[20] for MP-11 in solution ($E^0 = -100$ mV vs NHE); conversely, the E^0 for **MP-11b** is shifted 60 mV toward more positive values ($E^0 = -20$ mV vs NHE). The considerable shift of the E^0 value for **MP-11b** seems to indicate a different conformation of MP-11 deposited on the gold surface from the triply charged species.

The peak separation (ΔE_p) of **MP-11a** ($\Delta E_p = 45$ mV), lower than **MP-11b** ($\Delta E_p = 58$ mV), indicates a more reversible electrochemical behavior for MP-11 deposited from the $[MP\text{-}11 + H]^{2+}$ ions.

(20) (a) Wilson, M. T.; Ranson, R. J.; Masiakowski, P.; Czarnecka, E.; Brunori, M. *Eur. J. Biochem.* **1977**, *77*, 193–199. (b) Santucci, R.; Reinhard, H.; Brunori, M. *J. Am. Chem. Soc.* **1988**, *110*, 8536–8537.

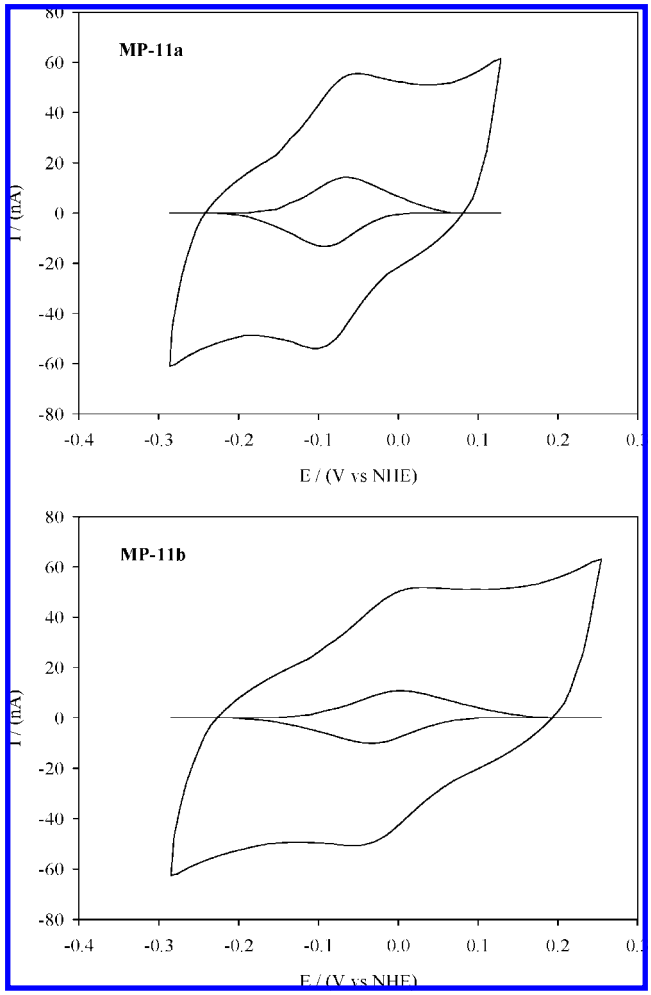

Figure 3. Cyclic voltammograms of **MP-11a** and **MP-11b** at a scan rate of 10 mV s^{-1} in 0.05 M PBS and 0.1 M KCl (pH 7.0) with N_2-saturated at 25 °C. The voltammograms are reported before and after background current, non faradic, subtraction. The dc bias applied potential is −70 V for **MP-11a** and −50 V for **MP-11b**. The time deposition is 90 min.

In Figure 4, the surface concentration of electroactive protein (Γ^*) on the gold electrode (considering an electrochemically available area of 0.9 mm^2), calculated by integration of the voltammetric anodic peak for **MP-11a** and **MP-11b** is reported as a function of the deposition time. Each point represents the mean value of at least five different determinations. The reproducibility of the soft-landed immobilization technique is ∼4%.

In the case of **MP-11a**, Γ^* attains a constant value for deposition times above 180 min, whereas **MP-11b** displays a similar behavior despite lower Γ^* values.

Considering a mean surface current of 100 pA measured for **MP-11a**, a total ion dose of 5.6 pmol is delivered to the surface after 180 min. By comparing this value with protein coverage obtained by cyclic voltammetry, an overall efficiency of the soft landing procedure of ∼8% is estimated.

Since the absolute intensities of the $[MP\text{-}11 + H]^{2+}$ and $[MP\text{-}11 + 2H]^{3+}$ ion are similar, a comparable ion dose of the triply charged species can be reached after a deposition time of 270 min. Moreover, the **MP-11b** Γ^* value is always lower than **MP-11a**, thus demonstrating a lesser soft-landing efficiency for the triply charged species.

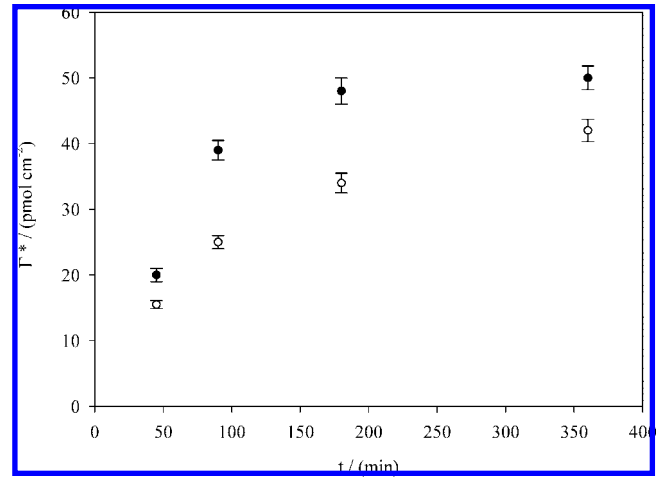

Figure 4. Behavior of electroactive protein concentration as a function of the deposition time for **MP-11a** (●) and **MP-11b** (○). Values were obtained by integrating the anodic peak from cyclic voltammetry experiments at a scan rate of 10 mV s^{-1} in 0.05 M PBS and 0.1 M KCl (pH 7.0) with N_2-saturated atmosphere at 25 °C.

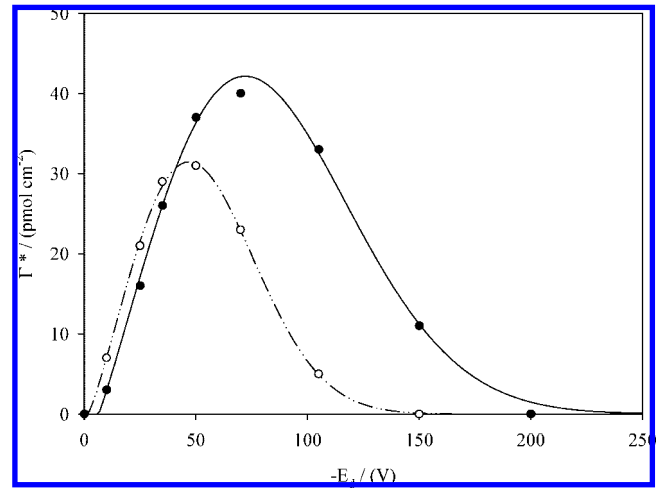

Figure 5. Concentration of the electroactive protein vs applied deposition potential for **MP-11a** (●) and for **MP-11b** (○). The ion deposition time is 90 min.

For deposition times longer than 90 min, the **MP-11a** voltammogram area decreases during the first scans, after which the area remains constant. This behavior seems to indicate that MP-11 deposited onto the gold surface is constituted by a strongly bound first layer onto which additional MP-11 molecules are weakly adsorbed and hence are rinsed off during the first voltammetric scans. Conversely, **MP-11b** shows a roughly constant voltammogram area due to a lower fraction of weakly bound MP-11, thus confirming its lesser deposition efficiency.

Reactive landing leads to the formation of the strongly bound MP-11 layer. It is worth noting that this layer maintains its redox activity for several days even after several consecutive voltammetric experiments in aqueous buffer solution.

In order to evaluate the contribution of the kinetic energy of the colliding ions to the immobilization process, a series of soft-landing experiments at different applied potentials (E_d) on the gold electrode surface were performed. In Figure 5, the concentration of the electroactive protein for **MP-11a** and **MP-11b** is reported as a function of the applied potential. An optimal deposition

potential of −70 V for **MP-11a** and of −50 V for **MP-11b**, respectively, is observed; hence, an optimal deposition potential for MP-11 may be estimated as 150 V/charge. The electrochemical properties of the deposited proteins are not significantly modified for E_d values close to the optimal deposition potential, whereas in the case of higher E_d values, a shift in the formal reduction potential (+50 mV for **MP-11a** and +20 mV for **MP-11b**) is observed.

As can be seen in the TOF-SIMS mass-resolved images, biasing the gold surface leads to the defocusing of the ion beam. This effect results in the coverage of the whole working gold electrode surface (12.6 mm^2), a spot size twice as large as the focused ion beam width, demonstrating that the ions can be guided by the applied potential to collide with a specific portion of the surface.

This peculiar feature of the soft-landing procedure may be used in the production of protein microarrays by considering the possibility of applying the dc potential to different spots on the same electrode surface.

In a control experiment, a drop of MP-11/phospate buffer solution was spread over the gold screen-printed electrode and dried in air. Only a weakly voltammetric current was measured during the first scan, which quickly disappeared. This suggests that the MP-11 linkage with the surface takes place upon collision and is promoted by the kinetic energy of the impinging ions.

The different electrochemical behavior of the two MP-11 ions soft landed onto the gold surface could be explained in terms of a difference in their interaction with the metal surface ascribed to the peptide chain. The pivotal role played by the peptide chain in the link with the gold layer is confirmed by several experiments performed by soft landing bare $[heme]^+$ ions at different applied potentials (50−100 eV). The absence of any voltammetric signal demonstrates that the heme group is not able to bind onto the metal surface.

The interaction of MP-11 ions with the gold surface should occur at the level of the protonated amino groups driven onto the surface by the negative potential applied to the working electrode. The contribution of the amino groups to the interaction between several molecules and the gold surfaces has been previously reported.[21]

Considering that the collision of ions with a clean metal target results in the neutralization of more than 99% of the projectile ions,[15c,d,22] the protonated amino group of **MP-11a** and **MP-11b** would reasonably be expected to be completely neutralized following their collision with the electrode.

In the light of the foregoing, the deposition of **MP-11a** with respect to **MP-11b**, which demands the loss of only one proton, should be facilitated. This may explain the higher yield of landed protein obtained by soft landing the doubly charged ion.

In addition, the interaction between **MP-11b** and the gold surfaces seems to be stronger than for **MP-11a**. This feature could be explained by considering a different gas-phase conformation for the $[MP\text{-}11 + H]^{2+}$ and $[MP\text{-}11 + 2H]^{3+}$ ions.

As previously demonstrated by Fornarini et al.,[23] who studied the gas-phase reactivity of $[MP\text{-}11 + H]^{2+}$ and $[MP\text{-}11 + 2H]^{3+}$ ions toward $OP(OMe)_3$, the doubly charged species is unreactive, whereas $[MP\text{-}11 + 2H]^{3+}$ undergoes the stepwise addition of three $OP(OMe)_3$ molecules. The authors account for this by hypothesizing that the relatively high charge status of $[MP\text{-}11 + 2H]^{3+}$ leads to an unfolded conformation in which the axial Fe−histidine interaction is lost. Thus, the interaction between the metal and the phosphate molecules is allowed. Conversely, an intramolecular solvation stabilizes $[MP\text{-}11 + H]^{2+}$, which retains its native structure and hence is almost unreactive toward the nucleophile.

It is well-known that the loss of the Fe−histidine interaction in the heme-containing enzymes causes a shift of the $E°$ potential to more positive potentials.[20a] The $E°$ potential of **MP-11b** shifting 60 mV toward more positive values confirms that $[MP\text{-}11 + 2H]^{3+}$ is characterized by an unfolded conformation. Conversely, $[MP\text{-}11 + H]^{2+}$ ions maintain the intramolecular metal coordination.

Hence, unfolded **MP-11b** is characterized by amino groups that are more readily available for interaction with the gold surface and could be more strongly immobilized on the electrode surface. Accordingly, **MP-11b** shows a less reversible electrochemical behavior than **MP-11a** since the likelihood of its taking on an orientation more favorable for the electron-transfer process could be prevented by its strong interaction with the metal surface.

As far as acceleration potential is concerned, the kinetic energy of the projectile ion is critical in controlling the ion−surface reaction. The ion−surface collision activates the surface, causing it to react with the projectile and promoting strong interactions that are probably kinetically hindered in solution. Nevertheless, at acceleration potentials higher than 100 V, the collision with the gold surface leads to the formation of an unfolded conformation also for **MP-11a,** as is evidenced by the shift of its $E°$ to more positive values.

Kinetic Analysis of Electron Transfer. The ET phenomena occurring in soft-landed protein modified electrodes can be accounted for by the Marcus theory. The redox protein directly bound to the electrode surface represents an almost ideal system, which is not influenced by the presence of immobilizing or entrapping agents: the electrochemical interaction thus undisrupted was studied to determine the main ET kinetic parameters. As exhaustively described in the Marcus theory, the rate of electron transfer increases exponentially with electrochemical driving force, reaching a maximum value when sufficiently high overpotentials[17] are reached. Reorganization energy (λ) can be determined by measuring the dependence of potential on the electron-transfer rate between the limiting value (k_{max}) and the rate constant at zero overpotential (k_0). The coupling of Marcus' theory for a nonadiabatic electron transfer[24] with the Fermi−Dirac distribution relative to the density of electronic states (DOS) at the Fermi level of the metal electrode results in the following equation for the redox reactions rate constant:[18,25,26]

(21) (a) Thomas, K. G.; Prashant, V. K. *J. Am. Chem. Soc.* **2000**, *122*, 2655–2656. (b) Tom, R. T.; Suryanarayanan, V.; Reddy, P. G.; Baskaran, S.; Pradeep, T. *Langmuir* **2004**, *20*, 1909–1914.

(22) (a) Dongre, A. R.; Somogyi, A.; Wysocky, V. H. *J. Mass Spectrom.* **1996**, *31*, 339. (b) Cooks, R. G.; Ast, T.; Pradeep, T.; Wysocky, V. H. *Acc. Chem. Res.* **1994**, *27*, 316.

(23) Crestoni, M. E.; Fornarini, S. *J. Biol. Inorg. Chem* **2007**, *12*, 22–35.

(24) Marcus, R. A.; Sutin, N. *Biochim. Biophys. Acta* **1985**, *811*, 265–322.

(25) Honeychurch, M. J. *Langmuir* **1999**, *15*, 5158–5163.

(26) Jeuken, L. J. C.; McEvoy, J. P.; Armstrong, F. A. *J. Phys. Chem. B* **2002**, *106*, 2304–2313.

$$k_{red/ox} = k_{max}\sqrt{\frac{RT}{4\pi\lambda}}\int_{-\infty}^{\infty}\frac{\exp\left(-\left(\frac{\lambda \pm F(E-E^{0'})}{RT} - x\right)^2\frac{RT}{4\lambda}\right)}{\exp(x)+1}\,dx \quad (1)$$

where $k_{red/ox}$ is the rate of electron transfer (in s^{-1}), E is the applied potential, E^0 is the formal reduction potential of the adsorbed couple, and λ (in J mol^{-1}) is the reorganization energy. For k_{red}, $x = (E - E_i)F/RT$ and for k_{ox}, $x = (E_i - E)F/RT$, E_i is the potential of the Fermi level in the electrode.

The k_{max} value can be calculated by the following equation:

$$k_{max} = \frac{4\pi^2}{N_A h} V_0^2\, e^{-\beta r}\frac{1}{RT} \quad (2)$$

V_0 (in J mol^{-1}) is the degree of electronic coupling, β (in Å) is the decay coefficient, and r (in Å) is the distance between centers.

The experimentally obtained cyclic voltammograms of **MP-11a** and **MP-11b** (deposition time 90 min, applied potential of −70 and −50 V, respectively) were modeled in order to calculate the rate of electron transfer and its change with the driving force by means of a finite difference procedure[18] using the Levenberg−Marquardt algorithm.[27] As discussed elsewhere,[26,28] the analysis of the experimental data has been simplified by correcting the simulation for (a) a slight modification of the formal potential $E^{0\prime}$ increasing the scan rate, (b) a constant peak separation at low scan rates (v), and (c) a half-height peak width that are broader than the theoretical value.

An increase in reduction and oxidation peak separation, as well as in peak width, is observed at increasing scan rates (Figures 6 and 7): both those behaviors agree with the Marcus model and are consistent with the kinetic limitation of electron transfer.[18] A relatively constant peak separation such as is found for the redox couple of **MP-11a** and **MP-11b** at low scan rates was observed in thin films of many redox proteins.[28,29] This is not related to kinetics but may result from conformational differences between oxidized and reduced forms of the proteins.[30] From a theoretical point of view, the maximum electron-transfer rate constant (k_{max}) can be inferred from the peak position obtained at high scan rates. The experimental determinations indicate the practical impossibility of obtaining k_{max} values knowing only the peak position; conversely, k_0 values can be obtained from the peak position.

The peak potential versus v data were modeled by keeping the value of k_0 constant in order to determine k_{max} and vice versa. The processing performed for **MP-11a** is reported in Figure 6 by way of example: In Figure 6A, three different values of k_{max} have been considered using the same fixed k_0 value and changing the λ value; conversely, in Figure 6B, three different values of k_0 have been considered using the same k_{max} value and changing λ. This procedure shows that the peak position is not sensitive to k_{max} within the peak separation range, whereas it is influenced by k_0, which can thus be calculated (see Table 1).

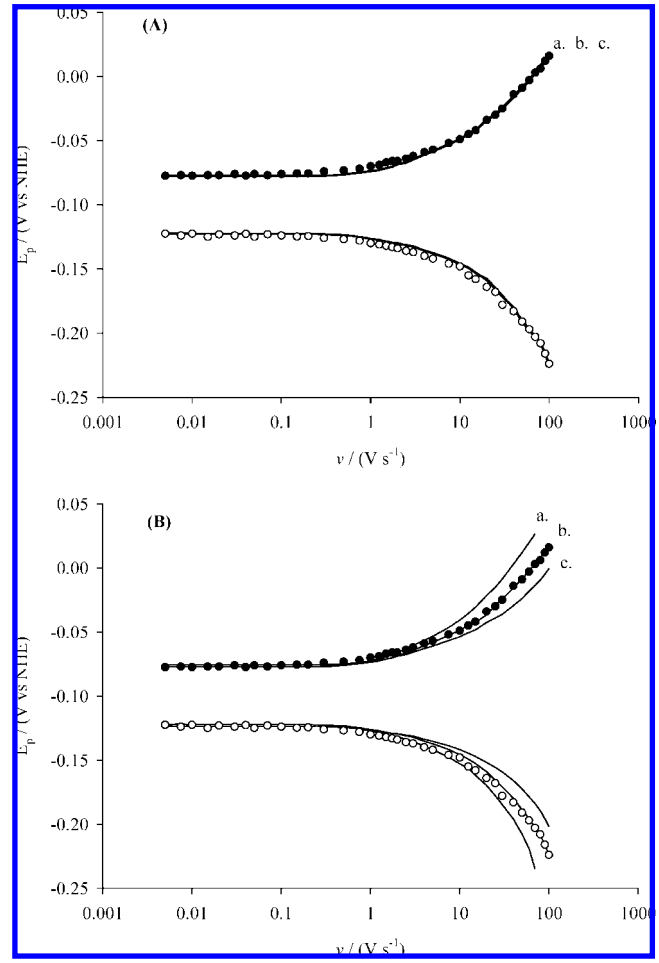

Figure 6. Anodic (●) and cathodic (○) peak potential as a function of the scan rate (log scale) for **MP-11a** in 0.05 M PBS and 0.1 M KCl (pH 7.0) with N_2-saturated atmosphere at 25 °C. The continuous lines indicate the results obtained in the simulation based on the Marcus theory in the following conditions: (A) $k_0 = 1080\ s^{-1}$, $E'^0 = -80 \pm 2$ mV; for $k_{max} = 10^6\ s^{-1}$; $\lambda \approx 0.8$ eV (curve a); $k_{max} = 10^8\ s^{-1}$; $\lambda \approx 1.1$ eV (curve b); $k_{max} = 10^{10}\ s^{-1}$; $\lambda \approx 1.4$ eV (curve c); (B) $k_{max} = 3 \times 10^7\ s^{-1}$, $E'^0 = -80 \pm 2$ mV; for $k_0 = 540\ s^{-1}$ (curve a); $k_0 = 1080\ s^{-1}$ (curve b); $k_0 = 1620\ s^{-1}$ (curve c).

In order to calculate k_{max}, a different approach[26] was followed, taking into account the variation of the peak width at the half-height peak with the scan rate (Figure 7). The peak width is higher than the Nernstian limit[31] (even in the case of low scan rates, i.e., <30 mV s^{-1}); hence, the peak width obtained from the theoretical model has been adequately corrected. The width surplus could be dependent either on the thermodynamic or the kinetic effects, which can hardly be differentiated.[32–34] The continuous line represents the simulation operated using the same

(27) Press, W. H.; Teukolsky, S. A.; Vetterling, W. T.; Flannery, B. P. *Numerical recipes in C,* 2nd ed.; Cambridge University Press: Cambridge, U.K., 1992.

(28) Jeuken, L. J. C.; Armstrong, F. A. *J. Phys. Chem. B* **2001**, *105*, 5271–5282.

(29) (a) Chen, X.; Ferrigno, R.; Yang, J.; Whitesides, M. *Lagnmuir* **2002**, *18*, 7009–7015. (b) Heering, H. A.; Wiertz, F. G. M.; Deeker, C.; de Vires, S. *J. Am. Chem. Soc.* **2004**, *126*, 11103–11112 (c) Rusling, J. F.; Zhang, Z. *In Biomolucules Films*; Rusling, J. F., Ed.; Marcel Dekker; New York, 2003; pp 1−64.

(30) El Kasmi, A.; Leopold, M. C.; Galligan, R.; Robertson, R. T.; Saavedra, S. S.; El Kacemi, K.; Bowden, E. F. *Electrochem. Commun.* **2002**, *4*, 177–181.

(31) Bard, A. J.; Faulkner L. R. *Electrochemical Methods,* 2nd ed.; Wiley: New York, 2002.

(32) (a) Clark, R. A.; Bowden, E. F. *Langmuir* **1997**, *13*, 559–565. (b) Kasmi, A. E.; Wallace, J. M.; Bowden, E. F.; Binet, S. M.; Linderman, R. J. *J. Am. Chem. Soc.* **1998**, *120*, 225–226.

(33) Rowe, G. K.; Carter, M. T.; Richardson, C. J.; Murray, R. W. *Langmuir* **1995**, *11*, 1797–1806.

(34) Léger, C.; Jones, A. K.; Albracht, S. P. J.; Armstrong, F. A. *J. Phys. Chem.* **2002**, *106*, 13058–13063.

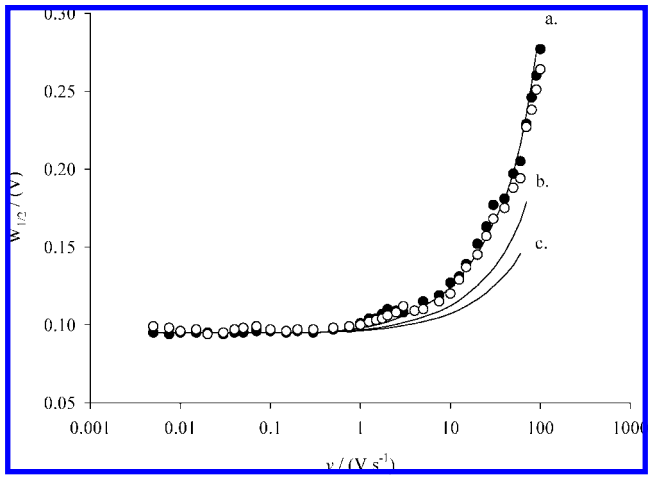

Figure 7. Anodic (●) and cathodic (○) peak half-height width ($W_{1/2}$) as a function of the scan rate (V s^{-1}) (log scale) obtained for **MP-11a** in 0.05 M PBS and 0.1 M KCl (pH 7.0) with N_2-saturated atmosphere at 25 °C. The continuous lines indicate the results obtained in the simulation based on the Marcus theory in the following conditions: $k_0 = 1080\ s^{-1}$, $E^{0'} = -80 \pm 2$ mV for $k_{max} = 10^6\ s^{-1}$; $\lambda \approx 0.8$ eV (curve a); $k_{max} = 10^8\ s^{-1}$; $\lambda \approx 1.1$ eV (curve b); $k_{max} = 10^{10}\ s^{-1}$; $\lambda \approx 1.4$ eV (curve c).

Table 1. Electron-Transfer Kinetic and Thermodynamic Properties of MP-11 Soft Landed on the Gold Surface

	$E^{0'}$ (mV vs NHE)	k_0 (s^{-1})	k_{max} (s^{-1})	λ (eV)
MP-11a	-80 ± 2	1080 ± 35	$(3.0 \pm 0.4) \times 10^7$	1.0 ± 0.1
MP-11b	-20 ± 3	810 ± 29	$(8 \pm 1.0) \times 10^5$	0.65 ± 0.08

parameters as applied in Figure 6; from this simulation it is possible to obtain k_{max} values (see Table 1).

Using the same approach, the main electrochemical parameters referring also to **MP-11b** were obtained and are shown in the same table (Table 1). It appears evident that measured k_0 values are considerably higher than those reported in the literature;[35] this behavior may be accounted for by considering that the direct electron-transfer kinetic parameters are actually generally influenced by both the protein interaction with the electrode surface and the resulting enzymatic layer structure.

Hence, when a redox protein is chemically immobilized using a SAM-like system[35,36] or is in any case physically entrapped,[37] the ET is eventually hindered due to the distance between redox center and electrode surface or to the presence of additional molecules. Otherwise, a system like a soft-landed protein surface proves to be characterized by a close contact between redox protein and the metal surface in the absence of any immobilizing matrix or tether molecules and hence ensures a fast electron transfer. From this point of view, the soft-landing procedure can be considered a promising tool to generate redox protein modified electrode surfaces characterized by efficient and fast electron transfer that is even better than the common immobilization procedure.

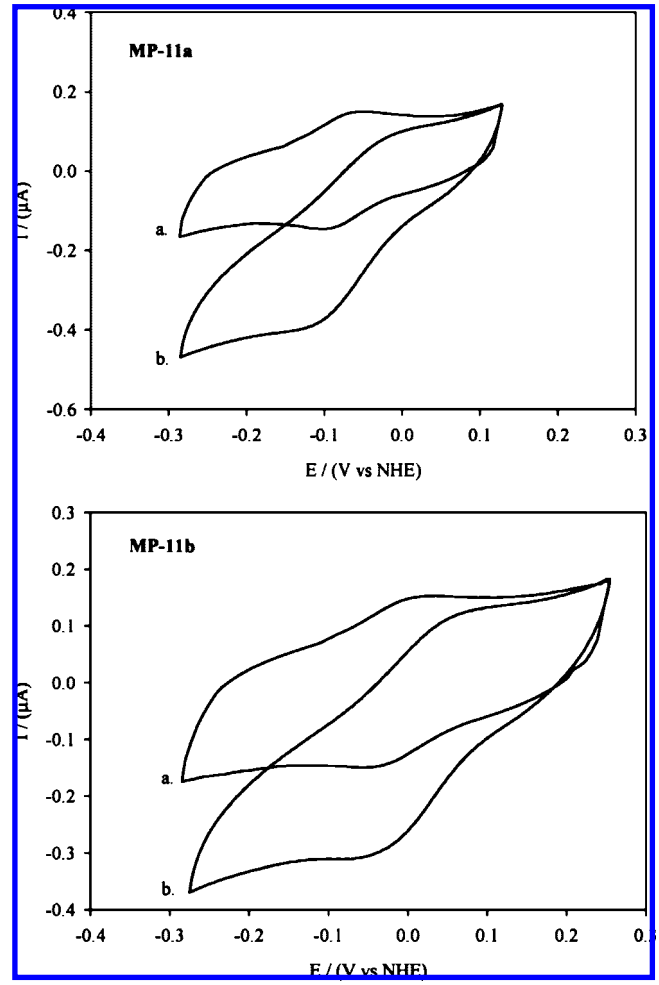

Figure 8. Cyclic voltammetry experiments obtained at a scan rate of 25 mV s^{-1} for **MP-11a** and **MP-11b**, in the absence (curve a) and in the presence of 0.08 mM H_2O_2 (curve b). The measurements were performed in 0.05 M PBS and 0.1 M KCl (pH 7.0) with N_2-saturated atmosphere at 25 °C. Deposition time: 180 min. Surface coverage: $(4.8 \pm 0.2) \times 10^{-11}$ mol/cm^2 for (MP-**11a**) (corresponding to ~90% of the electrode coverage) and $(3.4 \pm 0.1) \times 10^{-11}$ mol/cm^2 for (MP-**11b**) ions (corresponding to ~64% of the electrode coverage).

Another interesting aspect is the difference in the reorganization energy between **MP-11a** and **MP-11b**. This difference can be ascribed to the hypothesized different interaction of the two MP-11 ions and the electrode surface during the soft-landing reactive process. The lower value of the reorganization energy as well as of the electron-transfer kinetic constant calculated for **MP-11b** confirms our hypothesis about a stronger interaction of these species with the gold electrode surface (due to the higher availability of the amino groups thanks to its unfolded conformation, as stated above), which implies that the necessary (for ET) conformational changes of the protein are hindered. A comparison with literature values is not possible since the ET kinetics of MP-11 has not been fully characterized so far; in any case, experimental values of λ for the electron transfer of some other heme proteins (mioglobine, cytochrome *c* and cytochrome *b5*) have been reported in the literature.[38] In this case, an upper limit for the reorganization energy of 1.6 eV has been established, although

(35) Ruzgas, T.; Gaigalas, A.; Gorton, L. *J. Electroanal. Chem.* **1999**, *469*, 123–131.
(36) (a) Smalley, J. F.; Feldberg, S. W.; Chidsey, C. E.; Linford, M. R.; Newton, M. D.; Liu, Y. P. *J. Phys. Chem.* **1995**, *99*, 13141–13148. (b) Rivas, L.; Murgida, G. H.; Hildebrandt, P. *J. Phys. Chem. B* **2002**, *106*, 4823–4830.
(37) Wang, M.; Zhao, F.; Liu, Y.; Dong, S. *Biosens. Bioelectron.* **2005**, *21*, 209–214.
(38) Sharp, K. A. *Biophys. J.* **1998**, *74*, 1241–1250.

this value was determined using ruthenium-containing cofactors and thus represents the ET of the protein with a non-natural redox center. Further experiments have been performed with cytocrome *c* adsorbed on SAM electrode.[39,40] These studies indicate that the ET levels off at a driving force of 0.2−0.4 V and a good fit with DOS−Marcus theory was obtained using a reorganization energy close to 0.22 eV. This energy, much lower than that determined for **MP-11a** and **MP-11b**, may be ascribed to the exclusion of solvation molecules at the electrode−protein interface due to the shield effects of the large polypeptide surrounding the active site of cytocrome *c*.

Biological Activity. The catalytic activity of soft-landed MP-11 was investigated by cyclic voltammetry in the presence of H_2O_2 as substrate. Typical catalytic reduction peaks are shown in Figure 8, where catalytic turnover converts the peaklike signal (a) to a sigmoidal wave (b). The catalytic waves for the two-electron reductions of H_2O_2 to water are centered close to the **MP-11a** and **MP-11b** redox potential.

In the presence of H_2O_2 (P)Fe^{IV}−oxygen complexes are formed, which correspond to the so-called compounds I and II of horseradish peroxidase.[41] By increasing H_2O_2 concentration, the steady-state reduction peak current for both **MP-11a** and **MP-11b** increases linearly in the range 0.010−0.095 mM (for **MP-11a**) and 0.015−0.110 mM (for **MP-11b**).

A full analytical characterization of the two modified electrodes reveals a better performance for **MP-11a** than for **MP-11b**. This entails better conservation of biocatalytical properties for **MP-11a**, which again relies on a less denaturating soft-landing interaction with respect to **MP-11b**.

Beyond the linearity range, both calibration curves reach a maximum (probably ascribable to saturation of enzyme active sites); then, for $[H_2O_2] > 0.15$ mM, the catalytic current decreases significantly, suggesting a progressive inactivation of the enzyme (formation of compound III[41]). In any case, sensitivity is higher (for both **MP-11a** and **MP-11b**) than **MP-11** chemically or physically immobilized on electrode surfaces.[35,42] Finally, the soft-landed **MP-11** functionalized electrode displays a high stability (activity decreases by ∼10% over one week) and reproducibility, which ensure its suitability for practical applications such as biosensor transducer or cathodic elements in biofuel cells.

CONCLUSIONS

Soft-landed protein voltammetry is a new method based on the coupling of ion soft landing with voltammetric techniques. In the present report, we show for the first time that MP-11, soft landed on a gold electrode, is stable and retains its native properties and electron-transfer functionality. Our results afford fast, accurate, and exhaustive information about the immobilization yield of the deposited protein, the retention of its bioelectrochemical properties and the nature of the interaction between landed material and the surface. In particular, the existence of two conformations of the landed protein derived from two different ionic precursors and their strong interaction with the gold surface has been demonstrated.

Moreover, the main electron-transfer kinetic parameters were obtained by modeling cyclic voltammetry data. Calculated values of kinetic electron-transfer constant, formal redox potential, and reorganization energy indicate that the soft-landed protein surface is characterized by close contact between redox protein and the metal surfaces leading to a fast and reversible electron-transfer process. From this point of view, the soft-landing procedure seems to be a promising tool to create redox protein modified electrode surfaces characterized by efficient electron-transfer processes.

The science of proteins at electrodes is destined to produce some exciting future developments across a wide range of interests, spanning from the field of molecular electronics, multienzyme arrays, surface and interface science to nanostructures, catalysis, bioenergetics, and enzymology, provided that reliable efficient immobilizing procedures for redox proteins become available. To this end, SLPV should make an important contribution particularly in view of the key features demonstrated in this research, namely: (i) the possibility to select the molecular ion to deposit, (ii) the strong interaction with the surface although without protein denaturation, (iii) immobilization in the absence of any entrapping or tethering molecule ensuring an unmediated bridgeless efficient electron transfer, and (iv) the production of microarrays by driving different ions to specific surface portions.

ACKNOWLEDGMENT

Work carried out with the financial support of "Sapienza" University of Rome and of the European Commission under contract 017350 (BioMedNano). The authors express their gratitude to Ing. Renato Saviano for his contribution to mass spectrometer modification.

Received for review March 14, 2008. Accepted May 17, 2008.

AC8005389

(39) Murgida, G. H.; Hildebrandt, P. *J. Phys. Chem. B* **2002**, *106*, 12814–12819.
(40) Avila, A.; Gregory, B. W.; Niki, K.; Cotton, T. M. *J. Phys. Chem. B* **2000**, *104*, 2759–2766.
(41) (a) Hayashi, Y.; Yamazaki, I. *J. Biol. Chem.* **1979**, *254*, 9101–9106. (b) Farhangrazi, Z. S.; Fossett, M. E.; Powers, L. S., Jr *Biochemistry* **1995**, *34*, 2866–2871.
(42) (a) Tatsuma, T.; Mori, H.; Fujishima, A. *Anal. Chem.* **2000**, *72*, 2919–2924. (b) Komori, K.; Takada, K.; Tatsuma, T. *J. Electroanal. Chem.* **2005**, *585*, 89–96.